Journal of Harbin Institute of Technology (New Series), Vol. 19, No. 3, 2012

Ground substrates classification and adaptive walking through interaction dynamics for legged robots

SHAO Xue-song, YANG Yi-ping, WANG Wei

邵雪松, 杨一平, 王 伟

(Research Center of Integrated Information System, Institute of Automation, Chinese Academy of Sciences, Beijing 100190, China)

Abstract: Adaptive locomotion in different types of surfaces is of critical importance for legged robots. The knowledge of various ground substrates, especially some geological properties, plays an essential role in ensuring the legged robots' safety. In this paper, the interaction between the robots and the environments is investigated through interaction dynamics with the closed-loop system model, the compliant contact model, and the friction model, which unveil the influence of environment's geological characteristics for legged robots' locomotion. The proposed method to classify substrates is based on the interaction dynamics and the sensory-motor coordination. The foot contact forces, joint position errors, and joint motor currents, which reflect body dynamics, are measured as the sensing variables. We train and classify the features extracted from the raw data with a multilevel weighted k-Nearest Neighbor (kNN) algorithm. According to the interaction dynamics, the strategy of adaptive walking is developed by adjusting the touchdown angles and foot trajectories while lifting up and dropping down the foot. Experiments are conducted on five different substrates with quadruped robot FROG-I. The comparison with other classification methods and adaptive walking between different substrates demonstrate the effectiveness of our approach.

Key words: legged robot; ground substrates classification; adaptive walking; interaction dynamics

CLC number: TP242.3 **Document code**: A **Article ID**: 1005-9113(2012)03-0100-09

LEGGED robots has the superiority in walking on various challenging terrains in outdoor environments. Some terrains which contain slopes, holes, or other geometric obstacles can be easily detected by cameras, and the footholds can be selected rationally during dynamic locomotion[1]. Some other terrains, like sand, ice, snow, and soft soil, usually have flat surfaces, together with cameras' sensitivity to lighting variations, so it is difficult to capture their attributes[2]. Such non-geometric properties prevent legged robots from walking adaptively and safely, and low friction may lead to robots' slipping, and large damping may cause robots' stuck in the soft substrates, and small compliance may result in robots' vibration while contacting with the terrains. For this reason, the knowledge of geological properties can help to handle the problems in a more effective way, including adjusting control strategy among different terrains, and deciding whether robots should walk on or step back to keep safety towards a disastrous terrain. Therefore, methods for classifying the geological environments can facilitate the adaptive walking of legged robots. The most common approach for practical application is to group the terrains into classes rather than calculate their parameters accurately.

Geological sensing and classification has been widely researched in wheeled robots in past decades. Compared to the methods based on vision sensors and ladar sensors[3-4], the vibration-based classification was a hot topic in last few years, which is proposed by Iagnemma and Dubowsky in 2002[5]. Brooks et al. and Weiss et al. fixed accelerometers on the wheels or the bodies[2,6,8]. Giguere et al. put a single-axis accelerometer on the tip of a metallic rod dragged along surfaces behind a wheeled like robot[9]. Through analyzing the vibration signals from the accelerometers, some geological environments can be distinguished successfully from each other.

For legged robots, the contact dynamics is more complicated and some unpredicted random disturbances would arise while walking, so vibration-based geological sensing methods are not well suited. To test the terrain properties, Krotkov set a six-axis force-torque sensor at the end of a steel beam to simulate the leg of a six-legged walker[10-11]. Sinha and Bajcsy added a prototype foot with a compliant wrist sensor and a piezoelectric acceleration to a PUMA 560 robotic arm to work as the leg-ankle-foot system[12]. Recently, in Hopepflinger's research, a leg of the legged robot

Received 2011-10-12.

Corresponding author: WANG Wei, E-mail: wei.wang@ia.ac.cn.

ALoF was fastened to a base for testing[13]. The foot contact signal and the knee joint's motor current were measured through rotating the knee by ten degrees to classify the terrains with different surface friction. The above methods based on simplified testing platforms could get good results in certain conditions; however, they could hardly meet the requirements in real legged robots' locomotion.

Our primary work focuses on the classification method originated from interaction dynamics and sensory-motor coordination towards different ground substrates[14-15]. We consider the robot and the environment as a whole dynamic system. The interaction between them has an effect on the whole robot, including the position signals and current signals of motors at all joints, and the contact forces at all feet. Only a single-axis force sensor is needed to install at each foot. Considering the variation of body dynamics, contact forces, position errors, and motor currents from all legs are sampled while walking at different substrates at a constant speed. A multilevel weighted kNN algorithm is proposed to train the samples offline, and newly collected data can be classified online. Besides, adaptive control strategy is investigated through adjusting the touchdown angles and foot trajectories to deal with the change of substrates' properties. We present experimental results on the FROG-I (Four-legged Robot for Optimal Gaits) quadruped platform at five different ground substrates.

1 Interaction Dynamics

The interaction between robots and environments is modeled as a closed-loop system firstly. The closed-loop system model unveils the environments' influence to robots and gives some hints about how to make use of the interaction as a whole. As the most important environmental factors, impact and friction caused by ground substrate have crucial effects for legged robots' locomotion.

1.1 Closed-loop System Model

To simplify robots' control, a great emphasis is placed on the control of mechanical systems while ignoring environment conditions in traditional setting. The impacts caused by environments are usually considered as disturbance that is to be compensated to keep normal operation. When the influences become larger and unavoidable, control rules would be more complicated and in contrast, robots' operation performances would decrease sharply.

From the observation of legged robots' behaviors, we find that the coupling between a robot and its environment is an inevitable process. Furthermore, environments play positive roles in some aspects, for example, ground produces reaction forces on robots' legs to drive the robots moving forwards. Although ground substrates with different properties would bring negative effects on legs, they also provide opportunities to acquire the information as a feedback for better control at the same time[15-16]. Therefore, it is necessary to model a robot and its environment as a closed-loop system.

Dynamics system can be described as a differential equation,

$$\dot{x} = f(t, x), \ x \in \Omega \tag{1}$$

where $\Omega \in R^n$ represents the state space of the dynamics system and x is state variable of n dimensions. Now, the robot and the environment, parameterized as var_r and var_e respectively, are added in Eq. (1) in the following form

$$\dot{x} = f(t, x, \text{var\_}r, \text{var\_}e), \ x \in \Omega \tag{2}$$

With the initial condition, x_0, the solution of Eq. (2) is determined by the factors of var_r and var_e. The stable state, S, can be expressed as

$$S: = f_{t\to\infty}(x_0, \text{var\_}r, \text{var\_}e), \ x_0 \in \Omega \tag{3}$$

Hence, the relationship can be described clearly as with one of the two variables var_r and var_e kept unchanged; the system stable state corresponds to the other variable. In our geological environments classification, while behaviors of legged robots remaining unchanged, the observation variables reflect the variation of the ground substrates.

1.2 Compliant Contact Model

Assuming that robots' legs are rigid and contact time is small, compared to discrete contact models, continuous contact models, referred to as compliant contact models as well, explicitly reflect the viscoelasticity of the bodies during contact. Generally, three kinds of continuous models can be used to formulate the compliant contact dynamics. The linear Kelvin-Voigt contact model is a popular choice because of its simplicity; however, its energy inconsistency is not physically realistic. The original Hertz model is limited to contacts with elastic deformation and it does not account for energy exchange because damping is not considered[17]. To overcome the problems, the Hunt-Crossley model[18-20] was proposed with the contact force modeled as

$$F(t) = \begin{cases} \lambda x^p(t)\dot{x}^q(t) + kx^n(t), & x \geqslant 0 \\ 0, & x < 0 \end{cases} \tag{4}$$

where x is the penetration depth; $\dot{x}$ is the penetration velocity; k and λ are the elastic and viscous parameters of the contact, and n, p and q are real numbers that take into account the properties of contact surfaces. It is noticed that it is standard to set $p = n$ and $q = 1$.

The character of compliance c varies inversely with the elastic strength k as

$$c = \frac{\beta}{k}, \tag{5}$$

where β is the proportional factor.

The impact can be described with the coefficient of restitution, e, relating the relative normal velocity after contact v_o and the initial relative velocity v_i

$$e = -v_o/v_i, \tag{6}$$

The coefficient of restitution ($0 \leqslant e \leqslant 1$) meets the perfectly elastic impact ($e = 1$) and perfectly plastic impact ($e = 0$). For low impact velocities and materials with a elastic range, α can be used to characterize e,

$$e = 1 - \alpha v_i, \tag{7}$$

where α usually takes values below 1 s/m and equals to $2\lambda/3k$ with reasonable accuracy.

The contact occurs between a robot's leg and ground substrate, corresponding to an object of mass m contacting with a body of much greater mass. Therefore, the contact force can also be given by

$$F(t) = m\ddot{x}, \tag{8}$$

Considering the law of energy conservation, the initial kinetic energy, that the robot's leg possesses, is converted into two parts,

$$\frac{1}{2}mv_i^2 = \frac{1}{2}mv_o^2 + W, \tag{9}$$

where W is composed of elastic energy W_k and energy loss of damping W_λ. According to the definition of work-energy relationship, $W = \int F\mathrm{d}x$, W has the form as

$$W = W_k + W_\lambda = \int_0^t kx^n(t)\,\dot{x}(t)\,\mathrm{d}t + \int_0^t \lambda x^p(t)\,\dot{x}^q(t)\,\dot{x}(t)\,\mathrm{d}t, \tag{10}$$

At the end of the impact, the elastic energy is converted into final kinetic energy, and the initial energy is changed into output kinetic energy and dissipated energy.

1.3 Friction Model

The friction which causes slippage of legged robots is complicated to model. At present, friction models may be classified as static model and dynamic model. The static model relies on the relative velocity while the dynamic model is a function of both velocity and displacement[17]. In order to have more intuitive connection to actual physics, the static friction model is defined as

$$f = \begin{cases} f_e, & \text{if } |f_e| < f_{\max} \text{ and } v = 0 \\ f_{\max}, & \text{if } |f_e| \geqslant f_{\max} \text{ and } v = 0 \\ f_c + f_v + f_{\text{stribeck}}, & \text{otherwise} \end{cases} \tag{11}$$

where v is the relative velocity; f is the friction; f_e is the external force; $f_{\max}$ is the maximum static friction; f_c is the Coulomb friction; f_v is the viscous friction, and f_{stribeck} is the Stribeck friction which reveals the characteristic of moving at the beginning. Besides, f_c, f_v, and f_{stribeck} can be formulated as

$$f_c = \mu_c |f_N| \operatorname{sgn}(v), \tag{12}$$

$$f_v = \mu_v |v|^{\delta_v} \operatorname{sgn}(v), \tag{13}$$

$$f_{\text{str}} = (f_{\max} - \mu_c |f_N|)\, \mathrm{e}^{(\operatorname{sgn}(v) * (\frac{v}{v_{\text{str}}})^{\delta_{\text{str}}})} \operatorname{sgn}(v), \tag{14}$$

where μ_c is the kinetic coefficient of friction; f_N is the normal force imposed on the contact surface; μ_v is the viscous coefficient of friction; δ_v, v_{str} and δ_{str} are empirical constants, and $\operatorname{sgn}(\cdot)$ is the signum function.

2 Classification Method

2.1 Method Overview

The method based on interaction dynamics aims to classify the surfaces with different geological properties. This is in contrast to approach which depends on single sensor, like accelerometer or force sensor. Making use of single sensor usually can not capture the features completely and it may be out of use in some severe conditions. The proposed method believes that the interaction between the robot's legs and the ground substrate would have great influences on the whole robot. Through sensing body dynamics we could obtain the variation of states caused by ground substrates.

In our testing system, detecting variables are selected according to sensory-motor coordination derived from body dynamics[15]. The torsional stress, arising from contact force between one leg and the ground, affects the whole robot with slight deformation of the mechanical structure. To sense the variation of body dynamics, actuated motors at all joints can be taken as special sensors. Therefore, motor currents and position errors are detected as response to the impact. Furthermore, robots' legs can be used as probes with force sensors installed at each foot, since the contact forces at all feet would reflect the contact dynamics to some extent.

To collect useful information and reduce redundant data for training and classification, we divide one leg' walking period into four segments, stance phase, swing phase, colliding phase, and recovering phase. Colliding happens at the transition from swing phase to stance phase while recovering phase is the stage moving from stance phase to swing phase. From the analysis of interaction dynamics in Section II, the impact action and sliding effect, which play important roles on body dynamics, occurred at colliding phase and stance phase. Conversely, during swing phase and recovering phase, ground substrates have little interaction with the leg. For this reason testing happens at colliding phase and stance phase within each leg's walking period. In addition, time-scope of testing has to be of the same size at a constant speed. This makes the samples comparable with each other.

The collected raw data are transformed into representation composed of several kinds of features. Then,

a multilevel weighted kNN algorithm is designed to classify the new data online.

2.2 Feature Extraction

Each raw data vector v contains three kinds of testing variables, force signal v_f, position error v_e, and motor current v_c. $\{v_f\} = v_i, i = 1, \cdots n_1$, $\{v_e\} = v_i, i = 1, \cdots n_2$, $\{v_c\} = v_i, i = 1, \cdots n_3$, where n_1, n_2 and n_3 are the numbers of their sample times within the time-scope respectively. Fig. 1 shows two examples of raw data vectors for ground substrates of rigid rubber mat and soft foam mat. In each subplot, one curve's characters, such as mean, and variance etc, change a lot from the other. The common features for each vector of v_f, v_e, and v_c are listed as follows:

1) The mean μ.
2) The standard deviation σ.
3) The maximum $\max = \max(v_i)$, $v_i \in \{v_f, v_e, v_c\}$.
4) The minimum $\min = \min(v_i)$, $v_i \in \{v_f, v_e, v_c\}$.

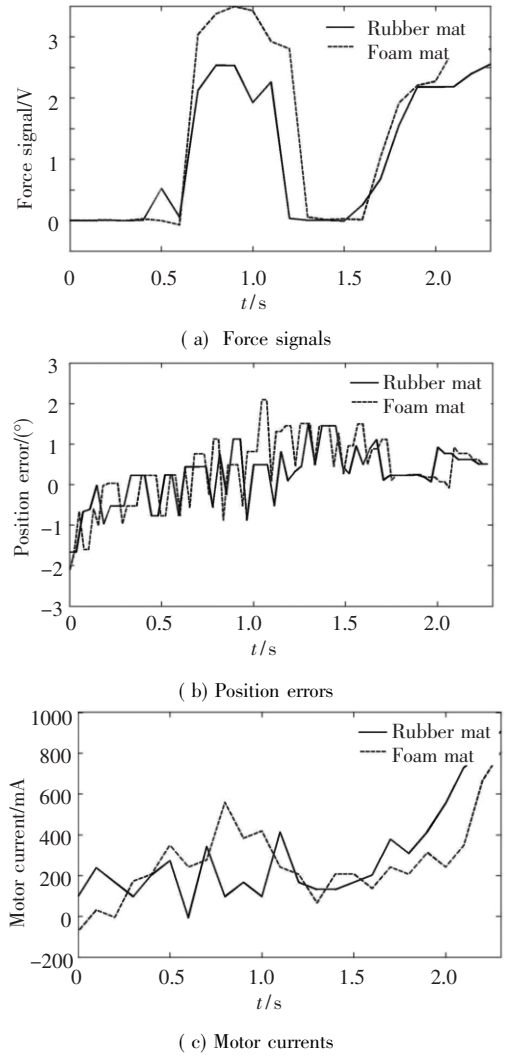

(a) Force signals

(b) Position errors

(c) Motor currents

Fig. 1 Two examples of raw data vectors for substrates of rubber mat and foam mat

To seek for useful information contained in raw data, some special features have to be selected towards different variables. For force signals, the number of values greater than 3V should be counted as k_f. With the increase of compliance and damping, the foot of legged robots would sink into the ground substrate to a certain extent, and the viscosity would prevent the foot from moving, so the contact force remains large for a fairly long time. The number of position errors greater than 1deg and the number of position errors less than -1deg also should be calculated as k_{e1} and k_{e2} separately, because slippery ground substrates can decrease the position precision. In addition, the thresholds selected here can be modified for different legged robots in ground substrates classification.

Through extracting from the raw data vector v, the features of force signals, position errors, and motor currents make up the feature vector s,

$$s = (s_{f1}, \cdots s_{fp}, s_{e1}, \cdots s_{eq}, s_{c1}, \cdots s_{cq}), \quad (15)$$

where p is the number of legs; q is the number of joints actuated by motors; $s_{f1}, \cdots s_{fp}$ are feature vectors of force signals; $s_{e1}, \cdots s_{eq}$ are feature vectors of position errors, and $s_{c1}, \cdots s_{cq}$ are feature vectors of motor currents. Furthermore, the vectors s_f, s_e, and s_c, which have five features, six features, and four features respectively, take the following form,

$$s_f = (\mu_f, \sigma_f, \min_f, \max_f, k_f), \quad (16)$$

$$s_e = (\mu_e, \sigma_e, \min_e, \max_e, k_{e1}, k_{e2}), \quad (17)$$

$$s_c = (\mu_c, \sigma_c, \min_c, \max_c), \quad (18)$$

2.3 kNN Classification

A multilevel weighted kNN classification algorithm is employed for dealing with the problem of geological environment classification. Compared with some complicated classifiers, the kNN algorithm is simple and easy to understand relatively; however, it usually has good performances in many cases[21].

First of all, the feature vectors of samples are labeled as corresponding known environments. All of them should be stored for training. The distances of a test vector to all training vectors should be calculated while classifying online. k feature vectors with smallest distances are selected as the result of that comparison. The test sample is belonged to the environment whose label has the highest occurrence frequency in the selected vectors. Besides, k is an empirical constant and its value is often chosen by trail and error.

The sensing variables play different effects on representing body dynamics, for instance, compared to position errors and motor currents, force signals directly reflect the behavior of impact. Thus, s_f, s_e, and s_c have different weights and the distance can be formulated as

$$d(u, v) = (\omega_1 \sum_{i=1}^{p} | y_{fi} - s_{fi} |^m +$$

$$\omega_2 \sum_{i=1}^{q} | y_{ei} - s_{ei} |^m + \omega_3 \sum_{i=1}^{q} | y_{ci} - s_{ci} |^m)^{1/m}, \quad (19)$$

where u is the test data vector; y_f, y_e, and y_c are variables' feature vectors; m is a positive integer. Moreover, for legged robots' ground substrates classification, it is difficult to get training samples, especially for the ground substrates with slippery surfaces or high compliance and damping. Therefore, larger weights are assigned to smaller distances to solve the problem of uneven distribution of the samples in different environments. This can be summarized as follows,

$$C_k(j) = \omega_k(j) \Gamma[d_j(u,v)] = \frac{k}{j} \Gamma[d_j(u,v)], \ j = 1,2,\cdots,k, \quad (20)$$

where $d_j(u,v)$ stands for the jth smallest distance; $\Gamma[d_j(u,v)]$ corresponds to the special known environment which the jth smallest distance belongs to; $\omega_k(j)$ is the weight to the special environment, and $C_k(j)$ is the final occurrence frequency of the known environment derived from the jth smallest distance. Meanwhile, collecting samples only at legs' colliding phases and stance phases reduces the required storage space and contributes to real-time calculation and classification.

3 Strategy of Adaptive Walking

It is widely known that the change of substrates' geological properties has been a great challenge for legged robots' adaptive walking. Many of them are limited to locomote on substrates with proper compliance and damping, as well as large enough coefficient of friction. To enlarge the range of application, legged robots must have the ability to adjust themselves to more complicated terrains.

In order to improve the stability, almost all of legged robots' legs are specially designed. The shanks of them always incline forwards, backwards, or sideways to extend support polygon while standing still and reduce needed torque while lifting up legs, such as Tekken robots[22], LittleDog[1], BigDog, etc. The direction of the resultant force, impacted on the foot, forms an angle θ with the vertical line(as shown in Fig. 2). The angle θ always changes in accordance with the touchdown angle ϕ, which is formed by the axis of the shank and the vertical line. As a result of relative motion, the power P_v is mainly needed to overcome viscous friction f'_v and Coulomb friction f'_c between the substrate and the immersed part of the foot while lifting up or putting down the leg. Frequently, the leg is moved along the direction of resultant force and P_v can be written as

$$P_v = (f'_v + f'_c) h/\cos\theta, \quad (21)$$

where h is the maximum distance below the surface of the substrate, f'_c and f'_v have the same form as Eqs. (12) and (13). Similarly, normal force $|F_n|$ and tangential force $|F_t|$ are respectively given by

$$|F_n| = |F| \cos\theta, \quad (22)$$

$$|F_t| = |F| \sin\theta, \quad (23)$$

Supposing that μ_s is the static coefficient of friction, and the maximum static friction $|f_{\max}|$ can be concluded as

$$|f_{\max}| = \mu_s |F_n| = \mu_s |F| \cos\theta, \quad (24)$$

If $|F_t|$ is bigger than $|f_{\max}|$, the foot would slip relatively to the ground substrate.

As the compliance and damping increase, the maximum penetration h and needed energy P_v get larger simultaneously. Then, θ can be reduced to prevent the increase of energy consumption of P_v according to Eq. (21). On the other side, if the substrate is more slippery, μ_s becomes smaller. To decrease the tangential force F_t as well as increase the maximum static friction $f_{\max}$, reducing the value of θ is also an effective approach from analysis of Eqs. (23) and (24). Therefore, ϕ and θ, which can be adjusted through planning of joint trajectories, are of critical importance in dealing with the change of geological properties.

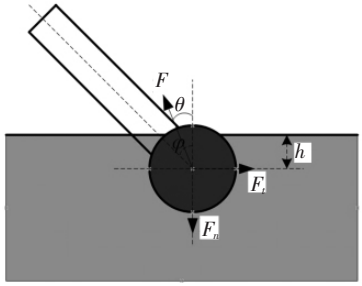

Fig. 2 Contact model with part of the foot below the ground substrate

4 Experimental Results

4.1 Experiments Setup

The quadruped robot FROG-I, shown in Fig. 3 (a), is about 1150 mm long, 700 mm wide, and 950 mm tall, with a total weight of approximately 55 kg. Each leg, known as the pitch-pitch type leg, contains one hip pitch joint and one knee pitch joint, both of which are powered by DC motors. Still, FROG-I possesses one passive compliant prismatic DOF at each toe which can be used to detect the contact between the foot and the ground. An embedded controller performs sensing and actuator control, and communicates with a Linux host computer through a wireless connection. The gyroscope, camera, foot contact sensors, and joint angle sensors have been installed on the quadruped robot.

Fig. 3(b) shows the structure of the foot in detail. There is a spring inside the moving part. When the foot collides with ground substrate, the prismatic joint moves upwards because of the ground reaction force. The foot contact sensor FSR is installed at the end of the moving part to detect the normal pressure impacted on the base. The bleeder circuit output different voltages as the resistance of FSR changes with the pressure.

(a) FROG-I robot

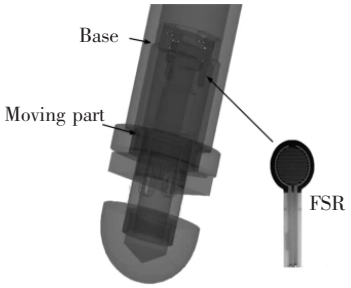

(b) CAD drawing

Fig. 3 FROG-I robot and 96/CAD drawing of the foot structure with foot contact sensor FSR(Force Sensing Resistor)

Five kinds of substrates with different compliance, damping, and friction were used in our experiments. The first kind is an emulsion polymerized styrene butadiene rubber (ESBR) mat and the second to the fifth are foam mats made up of polystyrene (PS), as shown in Fig. 4. From the first substrate to the fifth, they are marked as ESBR, PS1, PS2, PS3, and PS4 respectively.

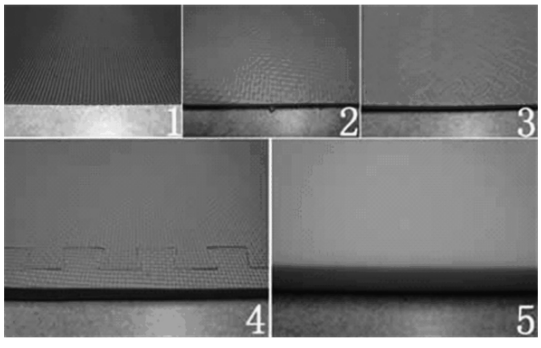

Fig. 4 Five kinds of substrates used in the experiments

According to FROG-I, a quadruped robot model was built in MSC. ADAMS[23]. Through simulating the five ground substrates as well as consulting the materials' properties, the parameters are estimated as shown in Tab. 1. Compliance, damping and viscous coefficient of friction increase while kinetic coefficient of friction and static coefficient of friction decrease from ESBR to PS4. Supposing the leg's mass $m = 7.5$ kg, the hysteresis loops are illustrated in Fig. 5 to analyze the contacts' characteristics. As c increases from 1.25e-005 to 1.667e-004 and λ increases from 2000 to 12000, the hysteresis loop is becoming bigger and the penetration is deeper, corresponding to the increase of dissipated energy.

Tab. 1 Substrates' parameters

	c (m/N)	λ (N·s/m^2)	μ_c	μ_v	μ_s
ESBR	1.111e-005	2000	0.50	0.2	0.80
PS1	2.000e-005	5000	0.30	1.0	0.50
PS2	2.174e-005	6000	0.28	1.1	0.45
PS3	3.333e-005	8000	0.25	1.6	0.40
PS4	1.667e-004	12000	0.16	10.0	0.27

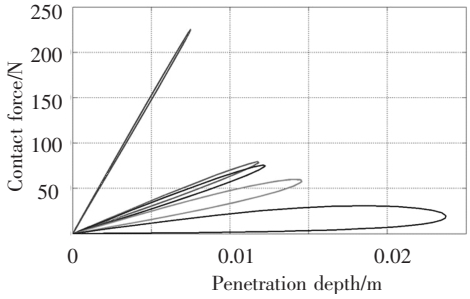

Fig. 5 Hysteresis loops for ESBR to PS4 (top to bottom loop)

4.2 Classification Results

In our experiments, the FROG-I robot walks on the five different ground substrates at a relatively low speed, roughly 0.06 m/s. The training samples are collected at each leg's colliding phase and stance phase of about 2.2 s. There are 41 samples for each substrate of ESBR, PS1, PS2, and PS3. Only 23 segments for the substrate of PS4 are sampled because of its poor suitability for normal walk. All of the samples are used for both of training and testing.

To verify the reliability and high efficiency of the proposed method derived from the whole body dynamics, three experiments are set and compared according to the results in Refs. [11] and [13]. The first one, named force signal method, only uses the force signals of the four feet as testing variables while the second one, named single leg method, makes use of the infor-

mation of only one leg, including force signals, position errors, and motor currents. All of the information of the four legs is utilized in the body dynamics method.

According to the multilevel weighted kNN algorithm, the weights of ω_1, ω_2, ω_3, and m in Eq. (19) are chosen as 0.6, 0.4, 0.4, and 2 respectively, and the classification results of three kinds of experiments for five different substrates are displayed in Fig. 6. The correct rates of value k from 2 to 10 are calculated to prove the method's robustness. For each k the average value of the five substrates' correct rates are extracted for the straightforward comparison of the three experiments. From Tab. 2 we can obviously find that, regardless of the value k, the body dynamics method has better performance compared with the other two methods. The best classification result occurs at $k = 3$ and the maximal average correct rate is 93.17%.

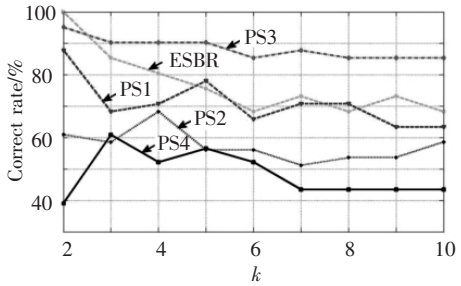

(a) Force signal method

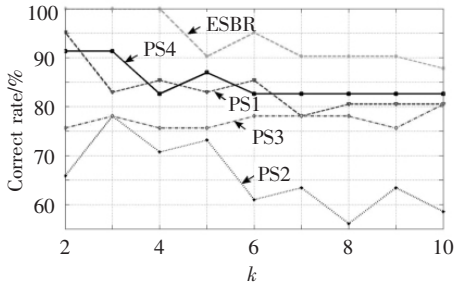

(b) Single leg method

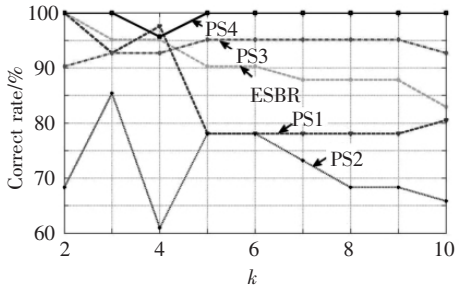

(c) Body dynamics method

Fig. 6 Classification results of correct rates from $k = 2$ to 10

Tab. 2 Average correct rates of the five substrates

k	Force Signal Method/%	Single Leg Method/%	Body Dynamics Method/%
2	76.61	85.58	91.71
3	72.66	86.07	93.17
4	72.39	82.86	88.40
5	71.30	81.78	88.29
6	65.56	80.42	88.29
7	65.28	78.47	86.83
8	64.31	77.50	85.85
9	63.82	78.47	85.85
10	63.82	77.99	84.39

For further discussion, the confusion matrix of classification result from the third experiment at $k = 3$ is shown in Tab. 3. The correct rates of PS1 and PS2 are relatively low and one of them is mostly misclassified as the other at the rate of 7.3%. The main reason of this is that the geological properties of PS1 and PS2 are close to each other. There are relatively small differences of body dynamics while walking on the two ground substrates.

Tab. 3 Confusion matrix of classification results

	ESBR	PS1/%	PS2/%	PS3/%	PS4/%
ESBR	95.1	2.4	0	2.4	0
PS1	0	92.6	7.3	0	0
PS2	7.3	7.3	85.3	0	0
PS3	0	7.3	0	92.7	0
PS4	0	0	0	0	100

4.3 Adaptive Walking

We test the proposed strategy of adaptive walking on the ground substrates of ESBR and PS4. The compliance, damping, and friction of them have the largest margins among the five ground substrates. ESBR has lower compliance, damping, and greater friction, which are suitable for normal walk. In contrast, the higher compliance, damping, and less friction of PS4 lead to feet' sticking and sliding easily.

In Fig. 7(a), while walking on the substrate of PS4, the foot trajectory's change rates at lifting up and dropping down phases become larger so that the touchdown angle ϕ becomes smaller to reduce the tangential force F_t, increase the normal force F_n, as well as decrease the energy consumption P_v. Because of the world coordinate system of each leg fixed at the hip joint, the leg's positions have negative values. In addition, the absolute values of the foot's positions change from 750 mm to 766 mm because the initial angels of hip joint and knee joint vary from walking on

ESBR to PS4 as shown in Fig. 7(b) . The definition of the hip angle is the angle between the vertical line and the axis of the thigh, and the knee joint angle is the angle between the axes of the thigh and shank. The initial hip joint angle changes from 15 degree to 8 degree while the initial knee joint angle changes from 28 degree to 14 degree corresponding to ESBR and PS4.

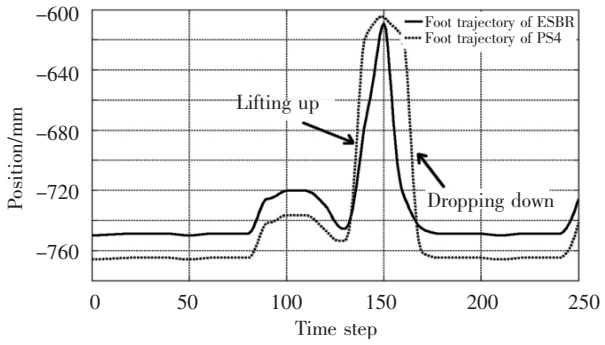

(a) Solid curve and dotted curve represent foot trajectories while walking on the substrates of ESBR and PS4 respectively

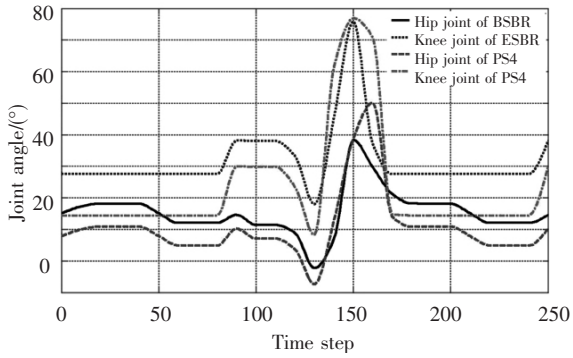

(b) Solid curve and dotted curve stand for hip joint trajectory and knee joint trajectory to ESBR, and dashed curve and dashdotted curve stand for hip joint trajectory and knee joint trajectory to PS4

Fig. 7 Right hind leg's foot trajectories and joint trajectories

Figs. 8 and 9 show the snapshots of FROG-I walking on the substrates of ESBR and PS4 periodically. The front four pictures, number 1 to number 4, belong to the first period, and the rest four pictures, number 5 to number 8, belong to the last period. Each picture shows the moving leg in swing phase and the legs' moving sequence is right front-left hind-left front-right hind within one period. The video clip is attached with this paper and it is also available on the website of Ref. [24]. It should be noted that as result of the legs' adjustment to the substrates with smaller friction coefficient and more compliance and damping, the touchdown angle θ almost remains low values while standing on the ground. As the normal force F_n increases, joint motors of each leg need larger torques to lift up the leg. So the joint motors of legged robots should have enough torques to satisfy the adjustments of adaptive walking on different ground substrates.

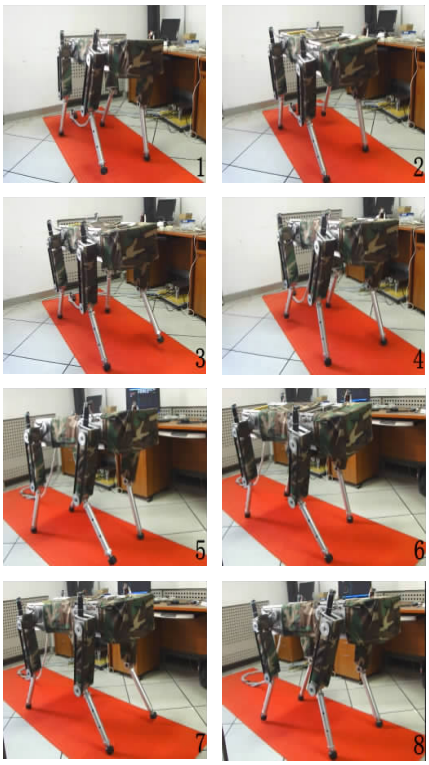

Fig. 8 Snapshots of adaptive walking on the substrate of ESBR

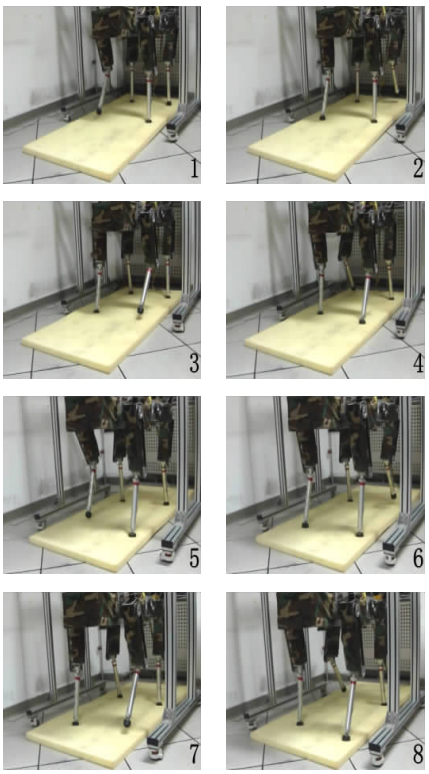

Fig. 9 Snapshots of adaptive walking on the substrate of PS4

5 Conclusions and Future Work

In this paper, we firstly proposed a novel ground substrates classification method based on legged robots' body dynamics. The interaction dynamics was modeled

to prove that geological properties, like compliance, damping, and friction, have significant influence on body dynamics. According to the sensory-motor coordination, position errors, and motor currents of all actuated joints are selected as sense variables. Together with forces signals at all feet, they are sampled during one leg's colliding phase and stance phase, and different features were extracted according to different variables. A multilevel weighted kNN algorithm, which solved the problem of uneven distribution of training samples, was used to classify different ground substrates. Then, through analyzing the interaction dynamics, we investigated a strategy of adaptive walking when the ground substrates became unsuitable for normal walk.

The experiments were conducted on the quadruped robot FROG-I. Our proposed body dynamics classification method was compared to the approaches with force signals or the variables of the moving leg addressed in Section V-B. The better results with k from 2 to 10 demonstrated the method's effectiveness and robustness. The best classification result occurred at $k = 3$, and the average correct rate was 93.17%. Besides, to adapt to the ground substrate with high compliance and damping, and low coefficient of friction, the initial angles of hip joints and knee joints were decreased while the vertical distances at uplifting and dropping down stages were increased through replanning foot trajectories to adjust the touchdown angles effectively.

Future work will be aimed at testing the proposed classification method and the strategy of adaptive walking in outdoor environments, such as ice, sand, snow, etc.

References:

[1] Kalakrishnan M, Buchli J, Pastor P, *et al*. Fast, robust quadruped locomotion over challenging terrain. Proceedings of IEEE International Conference on Robotics and Automation. Alaska: IEEE, 2010. 2665 - 2670.

[2] Brooks C A, Iagnemma K. Vibration-based terrain classification for planetary exploration rovers. IEEE Transactions on Robotics, 2005, 21(6): 1185 - 1191.

[3] Spinello L, Triebel R, Siegwart R. Multiclass multimodal detection and tracking in urban environments. The International Journal of Robotics Researchs, 2010, 29(12): 1498 - 1515.

[4] Vandapel N, Huber D, Kapuria A, *et al*. Natural terrain classification using 3-d ladar data. Proceedings of IEEE International Conference on Robotics and Automation. Barcelona: IEEE, 2004. 5117 - 5122.

[5] Iagnemma K D, Dubowsky S. Terrain estimation for high speed rough terrain autonomous vehicle navigation. Proceedings of the SPIE Conference on Unmanned Ground Vehicle Technology IV. Orlando: SPIE, 2002. 256 - 266.

[6] Brooks C A, Iagnemma K. Self-supervised classification for planetary rover terrain sensing. Proceedings of IEEE Aerospace Conference. Big Sky, Montana: IEEE, 2007. 1 - 9.

[7] Weiss C, Frohlich H, Zell A. Vibration-based terrain classification using support vector machines. Proceedings of IEEE/RSJ International Conference on Intelligent Robots and Systems. Beijing: IEEE, 2006. 4429 - 4434.

[8] Weiss C, Fechner N, Stark M, *et al*. Comparison of different approaches to vibration-based terrain classification. Proceedings of the 3rd European Conference on Mobil Robots. Freiburg. 2007. 7 - 12.

[9] Giguere P, Dudek G. Surface identification using simple contact dynamics for mobile robots. Proceedings of IEEE International Conference on Robotics and Automation. Kobe: IEEE, 2009. 3301 - 3306.

[10] Krotkov E. Active perception for legged locomotion: every step is an experiment. Proceedings of the 5th IEEE International Symposium on Intelligent Control. Philadelphia: IEEE, 1990. 227 - 232.

[11] Krotkov E. Robotic perception of material. Proceedings of International Joint Conference on Artificial Intelligence. Montreal: Citeseer, 1995. 88 - 95.

[12] Sinha P R, Bajcsy R K, Paul R P. How does a robot know where to step? Measuring the hardness and roughness of surfaces. Proceedings of the IEEE International Workshop on Intelligent Robots and Systems. Ibaraki: IEEE, 1990. 121 - 125.

[13] Hoepflinger M A, Remy C D, Hutter M, *et al*. Haptic terrain classification for legged robots. Proceedings of IEEE International Conference on Robotics and Automation. Alaska: IEEE, 2010. 2828 - 2833.

[14] Pfeifer R, Scheier C. Sensory-motor coordination: The metaphor and beyond. Robotics and Autonomous Systems, 1997, 20(2 - 4): 157 - 178.

[15] Iida F, Pfeifer R. Sensing through body dynamics. Robotics and Autonomous Systems, 2006, 54(8): 631 - 640.

[16] Johnson A M, Haynes G C, Koditschek D E. Disturbance detection, identification, and recovery by gait transition in legged robots. Proceedings of IEEE/RSJ International Conference on Intelligent Robots and Systems. Taibei: IEEE, 2010. 5347 - 5353.

[17] Gilardi G, Sharf I. Literature survey of contact dynamics modeling. Mechanism and Machine Theory, 2002, 37(10): 1213 - 1239.

[18] Marhefka D W, Orin D E. A compliant contact model with nonlinear damping for simulation of robotic systems. IEEE Transactions on Systems, Man, and Cybernetics, Part A: Systems and Humans, 1999, 29(6): 566 - 572.

[19] Diolaiti N, Melchiorri C, Stramigioli S. Contact impedance estimation for robotic systems. IEEE Transactions on Robotics, 2005, 21(5): 925 - 935.

[20] Haddadi A, Hashtrudi-Zaad K. A new method for online parameter estimation of Hunt-Crossley environment dynamic models. Proceedings of IEEE/RSJ International Conference on Intelligent Robots and Systems. Nice: IEEE, 2008. 981 - 986.

[21] Zhou L J, Wang L S, Ge X B, *et al*. A clustering-based KNN improved algorithm CLKNN for text classification. Proceedings of the 2nd International Asia Conference on Informatics in Control, Automation and Robotics. Wuhan: IEEE, 2010. 212 - 215.

[22] Kimura H, Fukuoka Y, Cohen A H. Adaptive dynamic walking of a quadruped robot on irregular terrain based on biological concepts. The International Journal of Robotics Research, 2007, 26(5): 475 - 490.

[23] Li B, Li X, Wang W, *et al*. A method based on central pattern generator for quadruped leg control. Proceedings of IEEE International Conference on Robotics and Biomimetics. Guilin: IEEE, 2009. 2035 - 2041.

[24] Shao X S, Wang W. Introduction of the FROG-I Quadruped Robot. http://irdc.ia.ac.rn/robot/,2012 - 06 - 01.